THE AMERICAN SOCIETY OF MECHANICAL ENGINEERS
345 E. 47 St., New York, N.Y. 10017

Dynamic Simulation of Compressor Station Operation Including Centrifugal Compressor & Gas Turbine

K. K. BOTROS
Nova Husky Research Corporation

and

P. J. CAMPBELL, D. B. MAH
Nova Corporation of Alberta
Calgary, Alberta, Canada

ABSTRACT

Dynamic simulation of the operation of a compressor station requires mathematical modelling of the dynamic behaviour of the compressor unit and various piping elements. Such models consist of large systems of non-linear partial differential equations describing the pipe flow together with non-linear algebraic equations describing the quasi-steady flow through various valves, constrictions and compressors. In addition, the models also include mathematical descriptions of the control system which consists of mixed algebraic and ordinary differential (mad) equations with some inequalities representing controllers' limits.

In this paper a numerical technique for the solution of the gas dynamics equations is described, which is based on the transfer matrix formulation relating the state vector time-difference at one side of an element to that on the other side. This approach facilitates incorporation of all elements transfer matrices into an overall transfer matrix according to the system geometrical connectivity. The paper also presents simulation results and comparison with actual field measurements of three case histories: 1) simulation of a compressor surge protection control process; 2) unit startup; and 3) slow transient of a compressor station responding to changes in the discharge pressure set point. Good agreement between simulation results and field measurements is demonstrated.

NOMENCLATURE

A	= pipe cross sectional area
c	= speed of sound
C_p	= specific heat at constant pressure
C_v	= specific heat at constant volume
D	= pipe inside diameter
E	= error
f	= Darcy friction factor (or function of)
F	= Function of U
G	= mass flow per unit area
H	= Function of U
H_p	= compressor polytropic head
k	= isentropic exponent
K	= proportional gain
LHV	= Lower Heating Value of fuel
$\dot{m}$	= mass flow rate
$\dot{m}_f$	= fuel mass flow rate
n	= polytropic exponent
N	= compressor speed
N_c	= normalization constant
N_G	= gas generator speed
P	= static pressure
Q_a	= actual inlet flow to compressor
[R]	= right-hand-side vector
s	= Laplace variable
t	= time
T	= absolute temperature
T_d	= derivative time constant
T_i	= integral time constant
[T]	= transfer matrix
u	= mean flow velocity
U	= state space vector
v	= specific volume
V	= volume
V_s	= bias
W_t	= turbine output power
x	= axial dimension
X	= position
y	= control signal vector
Z_a	= average compressibility factor

Greek letters

Δ	= forward difference
ζ	= damping coefficient
η_m	= mechanical efficiency
η_p	= compressor polytropic efficiency
η_t	= turbine thermal efficiency
θ,η	= two parameters in Beam & Warming Scheme
λ_i	= Runge-Kutta weights
ρ	= density
ξ	= pressure loss coefficient
τ	= time constant
ϕ_1,ϕ_2	= function defined in the text
ω_n	= natural frequency
$\alpha_1,\alpha_2,\alpha_3$	= constants

*Presented at the Gas Turbine and Aeroengine Congress and Exposition—June 11-14, 1990—Brussels, Belgium
This paper has been accepted for publication in the Transactions of the ASME
Discussion of it will be accepted at ASME Headquarters until September 30, 1990

Subscripts

a	= surrounding
n	= time step (n.Δt)
1	= section 1
2	= section 2
3	= section 3
oi	= stagnation condition at section i

INTRODUCTION

The technology relating to gas pipeline transient flow simulation is mature. Today, transient models of large gas pipeline networks for off-line purposes are generalized to the point that almost any practical network or straight line system can be readily simulated. The literature contains a vast amount of papers dealing with the subject of dynamic simulation of compressible gas flow in pipes. From an analysis point of view, these papers may be divided into two main categories; slow or rapid transients, for which formulations of the mathematical models are slightly different. Several different methods of solution for the pertinent one-dimensional conservation equations have been developed. The choice of a particular method is partly dependent upon the requirements of the system such as the degree of accuracy, size of the system, imposition of boundary conditions, variation of wave speed and the type of transient. A good review paper on the various numerical methods applied is by Thorley and Tiley [1].

The dynamic behaviour of the gas flow within a compressor station not only depends on the dynamic behaviour of each piping element, including the compressor itself, but also interacts strongly with the unit and station control system. The literature related to compressor station dynamic simulation including control systems are scarce. Some simulation programs exist already [2,3], but only for networks including compressor stations where the detailed dynamic behaviour of the control system is greatly simplified so as to observe only crucial set points and machine limitations. A rather practical model based on solving only the continuity and momentum equations coupled with the ordinary differential equations describing the control system was described in [4], and applied in chemical plants. Simplified dynamic simulation for the evaluation of new compressor controllers were performed by Van Zee [5]. Boyce et. al. [6] and Stanley and Bohannan [7] indicated the need for such coupling particularly at the design phase so as to assess the dynamic performance of the station and the effectiveness of its control system.

The work presented in this paper was motivated by this need. A computer program has been developed that deals with two levels of computations; a) the gas dynamics of the piping system, and b) the associated control loop response. The paper first describes briefly the mathematical models for the gas flow dynamics which consist of large systems of non-linear hyperbolic partial differential equations together with non-linear algebraic equations describing the quasi-steady flow through various valves, constrictions, compressors and their drivers. Secondly, a mathematical description of the control system which consists of mixed algebraic and ordinary differential (mad) equations with some inequalities representing controller's limits is presented.

Solution of the above two systems of equations is performed in a stepwise and sequential manner so as to close the feed back loop of information transferred between the two systems. Results and comparison with actual field measurements of gas recycling during the process of unit surge protection at a compressor test loop, and unit starup, are presented. The third example represents a slow transient of a variable speed compressor responding to changes in the discharge pressure set point.

GOVERNING EQUATIONS FOR YARD PIPING ELEMENTS

Straight Pipe

The general continuity, momentum and energy equations for one dimensional unsteady compressible fluid flow in a pipe can be written after some manipulation in the conservation form [8, 9]:

$$\frac{\partial U}{\partial t} + \frac{\partial F}{\partial x} + H = 0 \qquad (1)$$

where, U is the dependent state-space vector and F = F(U) , H = H(U) are both functions of U, viz.

$$U = \begin{bmatrix} \rho \\ \dot{m} \\ P \end{bmatrix}; \qquad F = \begin{bmatrix} G \\ G^2/\rho + P \\ \left(\frac{G}{\rho}\right)_n P + (c^2\rho)_n \left(\frac{G}{\rho}\right) \end{bmatrix};$$

$$G = \rho u = \dot{m}/A$$

$$H = \begin{bmatrix} 0 \\ \frac{f}{2D}\frac{G|G|}{\rho} \\ -\phi_1 \frac{G^2|G|}{\rho^3} \quad -\phi_2 \frac{T_a - T}{\rho} \end{bmatrix}; \qquad \phi_1 = \frac{f}{2DC_v}\left(\frac{\partial P}{\partial T}\right)_v$$

$$\phi_2 = \frac{4h}{DC_v}\left(\frac{\partial P}{\partial T}\right)_v$$

In reviewing the work of many authors on the solution of the above set of hyperbolic partial differential equations (P.D.E.), it is evident that the choice of a particular scheme or method of solution depends on the type of application. In the current application of compressor station dynamics, both slow and rapid transients can be anticipated. For example, transients caused by changes in compressor set points to meet certain demand requirements are considered slow. In this case, considerable savings in computational time and hence cost will be made by utilizing an implicit finite difference scheme which does not require a small time step for stability. However, if rapid transients are being considered, such as those caused by a compressor surge protection system, blowdown and startup/shutdown of unit(s), a small time step is required and a scheme such as Euler explicit finite difference may be satisfactory. We have, therefore, adopted the generalized time differencing scheme of Beam & Warming [10], which allows for the selection of various known schemes upon setting two independent parameters [Θ, η]. For example; for [Θ, η] equal to [0, 0], the Euler explicit scheme is invoked, while [1, 0] corresponds to Euler implicit; [1/2, 0] Crank-Nicolson; [1, 1/2] three-point backward; [0, -1/2] Leapfrog. The scheme, after linearization, can be put in a 'delta' form relating the change in the state vector ΔU_1 at one side (node) of a finite pipe element to the other side ΔU_2 (see Fig. 1a) via a [3x6] matrix [T], i.e.,

$$[T]\begin{bmatrix} \Delta U_1 \\ \\ \Delta U_2 \end{bmatrix} = [R] \qquad (2)$$

where,

$$\Delta U = U_{n+1} - U_n$$

and [R] is the right-hand-side vector of length [3x1]. Subscripts (n+1) and (n) refer to the time step indices. Both [T] and [R] are functions of the pipe geometrical dimensions, mean flow parameters, gas properties, and heat transfer parameters. This formulation of the

transfer matrix concept was necessary in order to facilitate integration of the elements transfer matrices into an overall transfer matrix according to the system geometrical connectivity between the various elements.

Constriction Elements

For flow constriction elements such as elbows, reducers, orifices and valves, a quasi-steady flow can be assumed at each time step of the numerical solution. The following equations can then be applied,

continuity: $$F_1 = \dot{m}_1 - \dot{m}_2 = 0 \qquad (3)$$

pressure loss equation:

$$F_2 = P_{01} - P_{02} - \xi\left(\frac{1}{2}\rho_1 u_1^2\right) = 0$$

$$F_2 = P_1\left[1 + \frac{k_1 - 1}{2}\left(\frac{\dot{m}_1}{\rho_1 A_1 c_1}\right)^2\right]^{\frac{k_1}{k_1-1}}$$

$$- P_2\left[1 + \frac{k_2 - 1}{2}\left(\frac{\dot{m}_2}{\rho_2 A_2 c_2}\right)^2\right]^{\frac{k_2}{k_2-1}} - \xi\left(\frac{\dot{m}_1^2}{2\rho_1 A_1^2}\right) = 0 \qquad (4)$$

energy equation: $$F_3 = h_{01} - h_{02} = 0 \qquad (5)$$

where subscripts 1 and 2 refer to upstream and downstream conditions of the element as shown in Fig. 1b, ξ is the pressure loss coefficient, k_1, k_2, c_1, c_2 are evaluated for the real gas from a state equation (BWRS or AGA-8 equations of state) at conditions 1 and 2.

Equations (3) through (5) can be linearized and put in a 'delta' form similar to that developed for a pipe [i.e. Eq. (2)] so as to be readily adaptable to the overall system transfer matrix. The first order Taylor expansion can be used which results in the following transfer matrix formulation:

$$\left[\frac{\partial F}{\partial U_1}, \frac{\partial F}{\partial U_2}\right]\begin{bmatrix}\Delta U_1 \\ \Delta U_2\end{bmatrix} = [-F]_n \qquad (6)$$

where F is the transposition of [F_1, F_2, F_3]; $\frac{\partial F}{\partial U_1}$ and $\frac{\partial F}{\partial U_2}$ are the Jacobian matrices evaluated at the time step (n.Δt). This formulation also leads to a [3x6] transfer matrix on the left-hand-side of Eq. (6).

In a similar manner, finite difference formulation based on a quasi-steady flow through various elements (Fig. 1) such as a volume element, e.g a station gas scrubber, combining and dividing Tee-elements, various types of valves, were developed [see ref.11].

GOVERNING EQUATION FOR TURBO MACHINERY

Variable Speed Centrifugal Compressor

The dual-shaft gas turbine/compressor arrangement is considered here, which is comprised of two basic functional sections: the gas generator and the power turbine, as shown in Fig. 1f. Although the speed of the gas generator (N_G) is different from that of the power turbine and compressor speed (N), it is closely associated

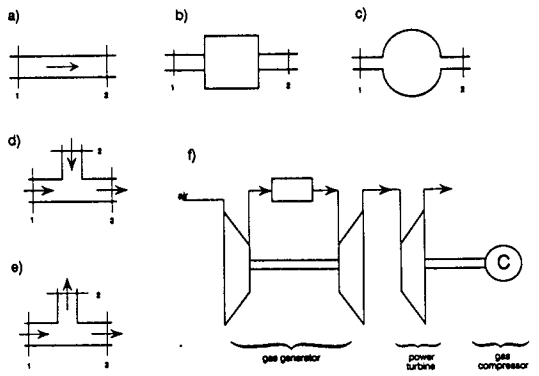

Fig. 1 Schematics of various gas piping elements.

with the power level required by the load. Both speeds are protected against overspeed by speed controllers. Modelling of this system requires attention and special consideration to the fact that there are two mechanically independent but thermodynamically coupled shafts.

In the following formulation, the compressor system is assumed to respond to any perturbation in a quasi-steady manner. Linearization via first order Taylor expansion with Jacobians evaluated at time (n.Δt) will be applied to the governing equations for both the centrifugal compressor and the gas turbine driver. This will furnish the relationship between the perturbed quantities of the gas flow on both sides of the compressor similar to that for other elements discussed above. The complication in the present formulation, however, arises from the introduction of the speeds (N) and (N_G) and the coupling between the compressor and the driver.

The governing equation of gas flow through the centrifugal compressor can be approximated by the polytropic process [12], i.e.,

continuity: $$F_1 = \dot{m}_1 - \dot{m}_2 = 0 \qquad (7)$$

polytropic pressure ratio:

$$F_2 = P_1/\rho_1^n - P_2/\rho_2^n = 0 \qquad (8)$$

polytropic head (energy):

$$F_3 = \frac{Z_a R T_1}{(n-1)/n}\left[(P_2/P_1)^{\frac{n-1}{n}} - 1\right] - H(Q_a, N) = 0 \qquad (9)$$

where the polytropic head (H_p) for the compressor is function of the actual inlet flow to the compressor (Q_a) and the compressor speed (N). A quadratic polynomial function was used alongside the affinity laws to determine H_p (Q_a, N) and also for the compressor polytropic efficiency η_p (Q_a, N), where η_p is defined as:

$$\eta_p = \left(\frac{n}{n-1}\right)/\left(\frac{k}{k-1}\right) \qquad (10)$$

and (n) is the polytropic index and (k) is the isentropic exponent at average suction and discharge conditions.

Linearization of the above equations results in:

$$\left[\begin{array}{c|c} \dfrac{\partial F}{\partial U_1}, \dfrac{\partial F}{\partial U_2} & \begin{matrix} 0 \\ 0 \\ \dfrac{\partial F_3}{\partial N} \end{matrix} \end{array}\right]_n \begin{bmatrix} \Delta U_1 \\ \Delta U_2 \\ \Delta N \end{bmatrix} = \begin{bmatrix} -F_1 \\ -F_2 \\ -F_3 \end{bmatrix}_n \qquad (11)$$

where F is the transposition of $[F_1, F_2, F_3]$ and the Jacobians $\frac{\partial F}{\partial U_1}, \frac{\partial F}{\partial U_2}$ and the right-hand-side vector are evaluated at the current time step (n.Δt).

For constant speed compressors, ΔN = 0, and hence the above equation reduces to the typical [3x6] transfer matrix formulation in the form:

$$\left[\frac{\partial F}{\partial U_1}, \frac{\partial F}{\partial U_2}\right]\begin{bmatrix} \Delta U_1 \\ \Delta U_2 \end{bmatrix} = \begin{bmatrix} -F_1 \\ -F_2 \\ -F_3 \end{bmatrix}_n \qquad (12)$$

which is a sufficient equation regardless of the driver. For a variable speed compressor, however, information regarding ΔN must be determined from the gas turbine performance characteristics as is shown below.

Gas Turbine

The power turbine output power (W_t), gas turbine overall thermal efficiency (η_t) or specific fuel consumption, exhaust gas temperature and inlet mass flow rate of air are all functions of the inlet air temperature and pressure, gas generator speed (N_G) and power turbine speed (N). For a given site condition, therefore, $W_t = W_t(N, N_G)$ and $\eta_t = \eta_t(N, N_G)$.

Gas turbine manufacturers usually furnish the above performance characteristics of the gas turbine either in a chart or empirical format. In the first case, it was found that cubic polynomial least square approximation of the performance characteristics of these two functions results in a good representation of the data when the following affinity laws were used,

$$\left(W_t / N_G^{\alpha_2}\right) = f\left(N / N_G^{\alpha_1}\right) \qquad (13)$$

$$\left(\eta_t / N_G^{\alpha_3}\right) = f\left(N / N_G^{\alpha_1}\right) \qquad (14)$$

where α, α_2, and α_3 are constants determined from two corresponding points (maximum power line) at two different N and N_G, for a given site condition.

Returning back to the requirement of determining ΔN in terms of gas flow perturbations (i.e. Eq. (11)), variation in compressor speed is connected to the fuel rate delivered to the gas turbine which is governed by the fuel control system. The power turbine output power (W_t) is related to the fuel rate ($\dot{m}_f$) and gas turbine overall thermal efficiency η_t viz,

$$F_4 = W_t(N, N_G) - \dot{m}_f(t).LHV.\eta_t(N, N_G) = 0 \qquad (15)$$

where LHV is the Lower Heating Valve of the fuel used. Linearization of the above equation at time (n.Δt) gives:

$$\left(\frac{\partial F_4}{\partial N}\right)\Delta N + \left(\frac{\partial F_4}{\partial N_G}\right)\Delta N_G = -F_4 \qquad (16)$$

where the Jacobian derivatives can be evaluated from Eqs. (13) and (14).

Furthermore, the machine matching between the compressor and the power turbine requires that the output power from the power turbine (W_t) times a mechanical efficiency (η_m) must be equal to the gas compressor power, i.e.

$$F_5 = \frac{H_p(Q_a, N).\dot{m}_1}{\eta_p(Q_a, N)} - \eta_m W_t(N, N_G) = 0 \qquad (17)$$

and linearization at time (n.Δt) gives:

$$\left(\frac{\partial F_5}{\partial \rho_1}\right)\Delta\rho_1 + \left(\frac{\partial F_5}{\partial \dot{m}_1}\right)\Delta\dot{m}_1 + \left(\frac{\partial F_5}{\partial N}\right)\Delta N + \left(\frac{\partial F_5}{\partial N_G}\right)\Delta N_G = -F_5 \qquad (18)$$

Equations (16) and (18) above can be solved together to determine ΔN and ΔN_G in terms of $\Delta\rho_1$ and Δm_1. The expression for ΔN can then be substituted in the compressor equation (11) to reveal the formal transfer matrix for the compressor in the normal form, i.e.,

$$[T]_c\begin{bmatrix} \delta U_1 \\ \delta U_2 \end{bmatrix} = [R] \qquad (19)$$

where $[T]_C$ is the required [3x6] compressor transfer matrix and [R] is the corresponding [3x1] right hand side vector. After the solution of the state-space vector U is obtained for the entire system at time (n+1)Δt, Eqs. (16) and (18) are then used to update the values of (N) and (N_G) at this time step.

It should be emphasized that the compressor and driver shaft inertias are neglected in the above formulation, and should be accounted for, particularly in relatively larger units. Other piping elements such as control valves, relief valves, conventional and non-slam check valves were also included in the simulation, but are omitted in this paper due to space limitation.

DYNAMIC REPRESENTATION OF THE CONTROL SYSTEM

In any realistic simulation of compressor station dynamics, the response of the control system and its control elements must be included. In the last section, the mathematical descriptions of the dynamic behavior of gas through various gas-handling elements and devices were presented. Typically, these elements are connected with some sort of autonomous control system whose behaviour is very important for any simulation of the flow transients.

The purpose of the station control system is to provide a collection of automatic functions so that the station operator may make major decisions, but not have to continually adjust the setting of a valve or the speed of each compressor unit, etc. Additionally, the control system permits remote operation from a central gas control location so as to provide overall operational integrity of the gas transmission network in an efficient and safe manner.

In the field, these functions are accomplished using a number of standard control elements such as: sensors, controllers, actuators, relays, ramp generators, filters, etc. All control circuits, whether pneumatic or electronic, can be described by a set of ordinary differential equations (O.D.E.) in the form:

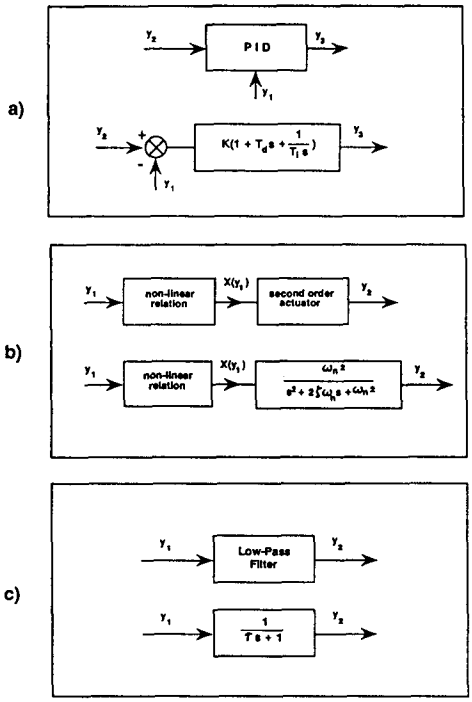

Fig.2 Schematics of basic control elements, and the corresponding Laplace transform.

$$\frac{dy}{dt} = f(y) \tag{20}$$

together with a set of subsidiary non-linear algebraic equations in the form:

$$F(y) = 0 \tag{21}$$

where (y) is a vector representing the state variable of measurements, control equipment and controllers' outputs, and F is the transposition of [F_1, F_2,...]. The following is a brief description of the basic control elements and the respective governing control equations.

P-I-D Controller

The output signal $y_3(t)$ from a P-I-D controller is related to the control signal $y_1(t)$ and the set point signal $y_2(t)$ (see Fig. 2.a) via the known equation:

$$y_3 = K\left[E + T_d\frac{dE}{dt} + \frac{1}{T_i}\int_0^t E\,dt\right] + V_s \tag{22}$$

where E = error = $(y_1-y_2)/N_C$

The derivative term in the above equation is approximated by a backward two-point difference form, while the integral term is approximated by the trapezoidal summation. This yields Eq. (22) above, a linear algebraic equation in y_1, y_2 and y_3.

Anti-reset windup is incorporated in the PID controller to help avoid problems related to saturation at the full limits of the controller output.

Dynamic Actuator/Positioner

The actuator is the part of a control loop that is attached directly to the station piping elements and adjusts the connected element setting in response to time-varying input signals from a controller, sensor or relay. Second order actuators are modelled by describing the varying relation between the actuator position X, input signal (y_1) and the actual position (y_2) (see Fig. 2.b) via:

$$\frac{d^2y_2}{dt^2} + 2\zeta\omega_n\frac{dy_2}{dt} + \omega_n^2[y_2 - X(y_1)] = 0 \tag{23}$$

where ζ and ω_n are the actuator constants (damping coefficient and natural frequency, respectively) which determine its response. The above second order ordinary differential equation can be converted into two first order ordinary differential equations in accordance with the system Eq. (20).

Low-Pass Filter

A low-pass filter provides a slowly varying output signal which tends asymptotically to the input signal. Examples of such control devices in the field are ramp generators and first order actuators. The rate of change of the output signal depends on the time constant (τ) of the filter. The equation which governs the relation of the output signal (y_2) to the input signal (y_1) (see Fig. 2c) is given by:

$$\tau\frac{dy_2}{dt} = (y_1 - y_2) \tag{24}$$

which is a first order ordinary differential equation.

The above three control elements constitute the basic building blocks for a variety of other control elements, filters, and compensators that can be found in the field. For example, a lead-lag filter or a lag-lead filter can be simulated by a PD controller and a ramp generator in series; a washout filter can be modelled as a differentiator (i.e. only the derivative component in a PID controller) and a ramp generator also in series. Once the Laplace transform of a control element is known, it is possible to construct from the building blocks of the above three basic elements the required model and proceed with the simulation. Other control elements such as comparators, multipliers,...etc. can be mathematically described by Eq. (21).

CLOSED LOOP SIMULATION

The mathematical description presented in the above three sections indicate that two levels of interconnected computations exist which must be solved either simultaneously in a parallel mode, or sequentially. The first level is the gas dynamics part of the flow-handling piping system in the compressor station. This level of computation involves a solution of a set of mixed non-linear P.D.E. and algebraic equations with appropriate boundary conditions and elements setting dictated by the control system. The other level of computation solves the dynamic behaviour of the station control system which involves a set of mixed non-linear algebraic and O.D.E. together with boundary conditions represented by set points and measured quantities. Figure 3 illustrates schematically the closed loop simulation of these two levels of computations. In the present work, computations were performed sequentially, although parallel computer techniques can lend itself quite well in this application.

The basic framework for the simulation model adopted for the piping system is the nodal approach, in which the system is said to be comprised of nodes and elements connecting these nodes. The relationship between the state space vector on each side of each

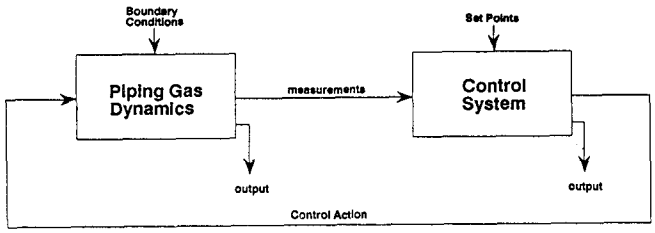

Fig. 3 Closed-loop dynamic simulation process.

element is formulated in a 'delta' form using the concept of the transfer matrix (see Eq. 2) and properly pooled in the system overall transfer matrix relating all space vectors at all system nodes. An effective solution technique which takes advantage of the sparse characteristics of the system matrix was implemented. The technique is based on a sparse variant of Gaussian elimination for the solution of unsymmetrical systems of equation [13]. The system of equation is closed by proper description of the number and type of boundary conditions in accordance with the system characteristics equation for the hyperbolic type of P.D.E.

As for the control system, solution of the mixed algebraic and ordinary differential equations (Eq. 20 and 21) is required. In the literature one finds very few algorithms for solving numerically such systems. One method [14] is to transform the algebraic equations into O.D.E. which, combined with the original O.D.E. can be solved relatively easily by standard numerical techniques. Another method stems from the multivalue method proposed by Gear [15], which replaces the system of the mixed equations by a system of purely algebraic equations obtained by substituting the finite difference approximations for all of the derivative terms. In the present work, simple m-stage Runge-Kutta method of the following form was considered for the part of equations represented by Eq. (20):

$$y_{n+1}^{(1)} = y_n + \lambda_1 \cdot \Delta t f(y_n)$$

$$y_{n+1}^{(2)} = y_n + \lambda_2 \cdot \Delta t f(y_{n+1}^{(1)})$$

$$y_{n+1}^{(r)} = y_n + \lambda_r \cdot \Delta t f(y_{n+1}^{(r-1)})$$

$$y_{n+1} = y_n + \Delta t f(y_{n+1}^{(m-1)}) \qquad (25)$$

where subscripts n and n+1 denote time levels, superscript denotes stage number, and λ_r are the Runge-Kutta weights. Notice that each stage has the form of the explicit Euler method advancing the dependent variable from $y_{n+1}^{(r-1)}$ to $y_{n+1}^{(r)}$ with time step size $\lambda_r \Delta t$. The weights λ_r may be chosen in a variety of ways, either to maximize accuracy, the size of the stability region, or a combination of both. In the present application, it is better to maximize the size of the stability region while keeping the order of approximation to first order. Van der Houwen [16] calls this class "stabilized Euler formulas" and gives the expressions defining the weights. For example, the weights for a four-stage solution are:

$$\lambda_1 = 1/64;\ \lambda_2 = 1/20;\ \lambda_3 = 5/32 \text{ and } \lambda_4 = 1.$$

As for the other part of the control system equations represented by the non-linear algebraic equations (21), a first order Taylor expansion was assumed; i.e.

$$F(y_n) + \left(\frac{\partial F}{\partial y}\right)_n (y_{n+1} - y_n) = 0 \qquad (26)$$

The above set of Eqs. (25) and (26), form a sparse system of linear equations which were also solved by the sparse variant of Gaussian elimination technique for the solution of unsymmetrical systems of equations resulting from the network type of the control systems.

A computer program (TRAN) has been developed which incorporates the above techniques and methods of solution. The program is PC-based and features user friendly interfaces for preprocessing, execution monitoring, and post processing.

SIMULATION RESULTS AND COMPARISON WITH FIELD MEASUREMENTS

The following are three examples of dynamic simulation of a compressor station during transient operation. The examples are taken from compressor stations in the gas transmission system of NOVA CORPORATION OF ALBERTA. The first two examples represent rapid transients during and compressor surge protection and startup, while the third demonstrates a slow transient of a compressor station responding to changes in the discharge pressure set point.

i) Compressor Surge Protection Control

This example involves field measurements of a single unit compressor station, the layout of which is shown schematically in Fig. 4. The objective was to assess the effectiveness of the surge protection control system as the field personnel indicated that the recycle valve tends to oscillate violently (from 0 to 50% open) when the compressor operates close to the surge control line. A field test was conducted and measurements were taken while the compressor was running at approximately constant speed of 18000 rpm. The station suction and discharge valves were used to throttle the flow and thereby bring the compressor operating point towards the surge region. Measurements of the suction and discharge static pressures and temperatures, and differential pressures across the suction side annubar and the discharge side orifice meter were recorded. Recycle valve position was also observed during the test. The measured data are plotted in indicative Figures 5 for a period of 100 seconds taken during operation at the surge control line while the surge protection control system was activated. Obviously, this surge control system is shown to be unstable as manifested by the pressure and flow oscillations (Fig. 5a and 5c, respectively) and the resulting cyclic behaviour on the compressor performance map (Fig. 5d). Dynamic simulation of the station with its control system was performed using TRAN. The surge controller was a PI controller whose settings at the time of the test were K = 5.0 and T_i = 1/9.5 seconds. With these settings and system boundary conditions, the simulation resulted in a remarkably good agreement with the field measurements as is demonstrated by corresponding Figures 6. The recycle valve position

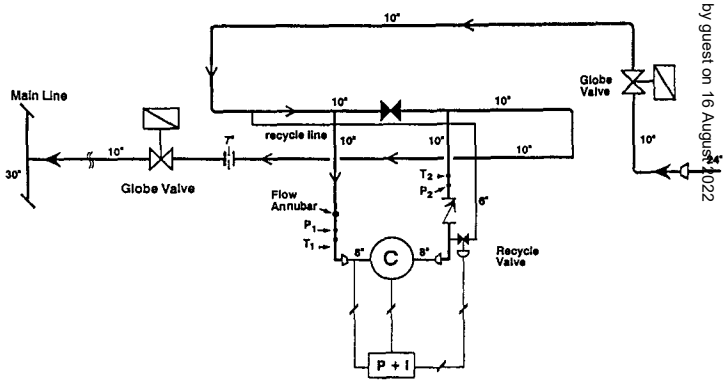

Fig. 4 Schematic of a single unit compressor station.

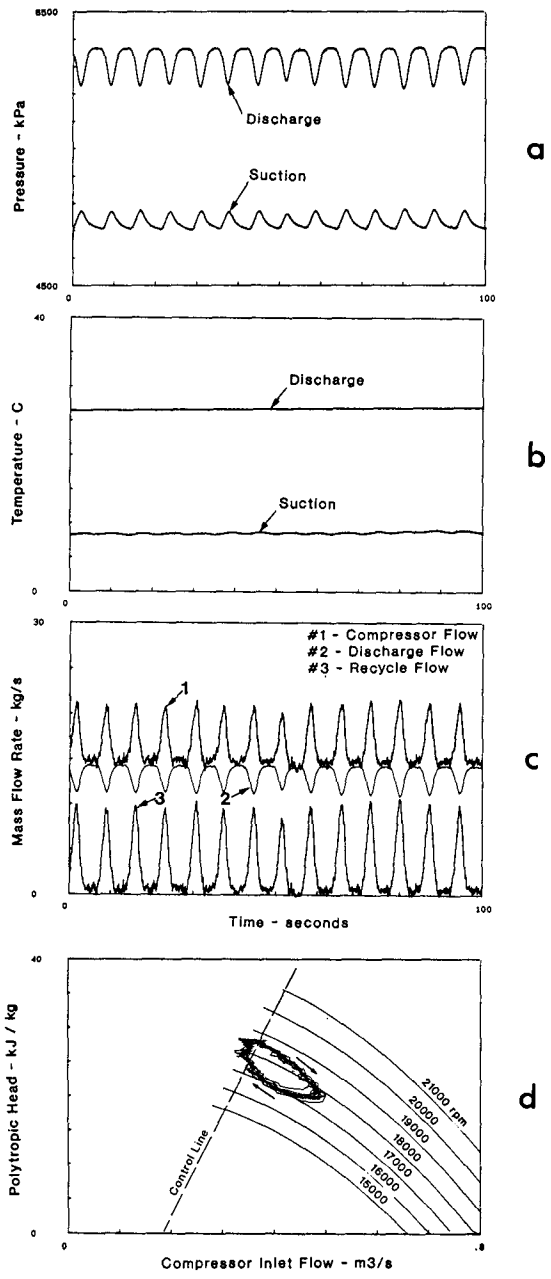

Fig. 5 Field measurements during the process of compressor surge protection of the system shown in Fig. 4.

(Fig. 6e) shows oscillations between ≈ 0-50% open as has been observed during the test but was not measured and recorded due to lack of valve position indicator on the valve. Although pressure, and flow oscillations both through the compressor and the recycle line, agree very well with those measured in the field, the temperature oscillations predicted by the simulation do not agree with those measured (compare Fig. 5b and Fig. 6b). This is due to the slow dynamic response of the temperature gauges placed in relatively high thermal capacitance jackets. However, the mean temperatures agree very well in both cases.

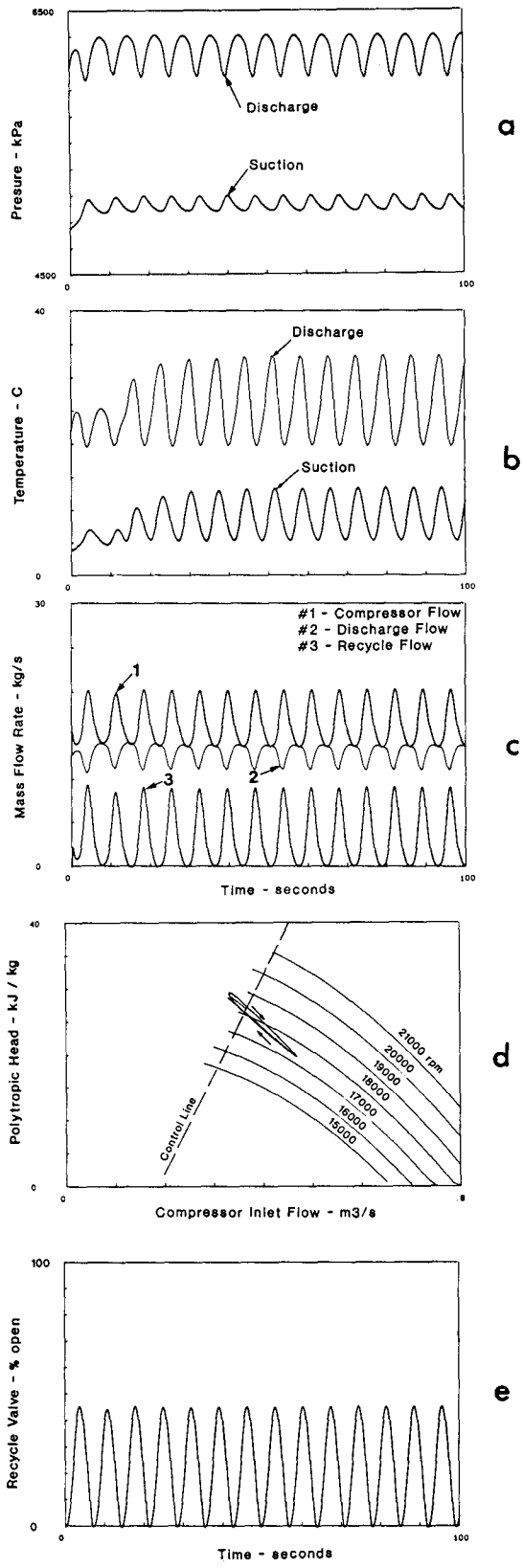

Fig. 6 Simulation results during the process of compressor surge protection of the system shown in Fig. 4.

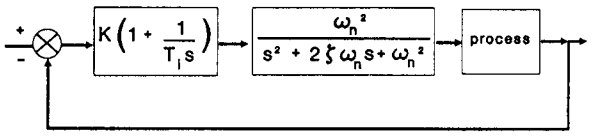

Fig. 7 Closed loop representation of the surge control system of Fig. 4.

The constants representing the damping coefficient (ζ) and natural frequency of the actuator (ω_n) of the recycle valve had to be estimated from the simplified control feedback loop shown in Fig. 7. In this feedback loop, the transfer function of the process representing the piping dynamics is assumed unity with respect to flow and pressure only and not to temperature. The open loop transfer function of the feedback loop represented in Fig. 7 is:

$$K\left(1+\frac{1}{T_i s}\right)\left(\frac{\omega_n^2}{s^2+2\zeta\omega_n s+\omega_n^2}\right)$$

while the root locus of the closed loop system is determined from solving the characteristic equation:

$$T_i s^3 + 2T_i\zeta\omega_n s^2 + (K+1)T_i\omega_n^2 s + K\omega_n^2 = 0$$

Since measurements were showing steady oscillation at a period of 7.2 seconds (see Fig. 5c), i.e., at frequency ω = 0.873 rad/s, then two roots of the characteristic equation must be $\pm$ iω. Equating both real and imaginary parts of the left-hand-side of the equation to zero yields

$$\omega_n = 0.356 \text{ and } \zeta = 11.12$$

for K = 5.0 and T_i = 1/9.5 seconds. The root locus of the feedback control loop shown in Fig. 7 is plotted in Fig. 8, where the three poles of the open loop transfer function are located at 0.0, -0.0161 and -7.9005. Only the first two poles are shown in Fig. 7 since the third one goes to the zero at $-1/T_i$, i.e., to -9.5 and hence has no influence on the control loop stability. The root locus plot of Fig. 8 indicates that stability will improve for a value of gain less than 5.0, and the lower this value, the higher damping that will be achieved. A value of K = 0.5 was therefore chosen and introduced to TRAN for full dynamic simulation. The results obtained confirmed the above analysis and are shown in corresponding Figures 9. Remarkable damping and suppression of oscillations were also achieved in the field with this lower value of K. The results of a subsequent field test (with K = 0.5) are shown in Fig. 10.

This example demonstrates that small adjustment of the PI controller can lead to a remarkable improvement in the control process. Full dynamic simulation is useful in selecting the appropriate parameter(s) to adjust in order to achieve best results, before final implementation is executed in the field.

ii) Compressor Startup

In normal operation of a gas compressor station, a unit can be started either manually or remotely with automatic valve sequencing. Typically after purging and pressurizing the compressor casing to the suction pressure, the unit suction, discharge and recycle valves are opened and the starter is switched on, accelerating the compressor to an idle (warmup) speed. When the gas turbine cumbustion pressure reaches a certain pressure, the starter drops out. After a warmup period, the compressor speed is then ramped up to a higher speed. At a certain speed the recycle valve is closed, allowing the unit

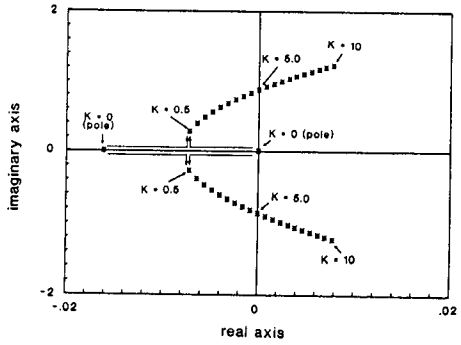

Fig. 8 Root locus of the closed loop control system of Fig.7.

discharge pressure to increase to a pressure slightly higher than the line discharge pressure at which point the unit check valve will open.

Simulation of the startup period form idling to on-line conditions for the compressor set of Fig. 4 was performed and compared to actual filed measurements. During testing, the discharge line pressure was only 55 kPa higher than the suction pressure, and therefore during idling at speed = 9400 rpm, the unit check valve was open allowing gas to flow to the discharge line as well. Figure 11 presents comparisons between simulation results and actual field measurements during 100 seconds covering the ramp up period. Prior to time zero and up to 25 seconds in Fig. 11, the compressor was idling at 9400 rpm, after which a ramp signal at a rate of 50 rpm per secomd was issed to the ramp generator. At time 80 seconds, another signal was issued to close the recycle valve while ramping continued.

Applying the above two signals (ramping and recycle valve closure) to the unit fuel system resulted in the fuel rate profile shown in Fig. 11a from the simulation. Comparison with field measurements of suction and discharge pressures and temperatures, compressor and recycle flows are shown in Fig. 11b, Fig. 11c, and Fig. 11d, respectively. Plot of the process on the compressor performance map is followed in Fig. 11e.

Good agreement between simulated results and measurements is demonstrated except for the temperature profiles. This is again due to the thermal capacitance of the thermal wells in which the temperature probes are placed.

iii) Compressor Station Set Point Change

Compressor station dynamic operation during slow transients has been simulated by TRAN and the results were compared with actual field measurements from telemetered data at one of Nova's compressor stations. The station contains two compressor units in series as shown in Fig. 12. For the comparison period, only unit #1 was running. Mainline flow conditions were relatively stable at far upstream (approx. 82 km). A flow controlled meter station is located approximately 66 km downstream of the compressor station where the flow demand during a six hour period is shown in Fig. 13 b. The flow demand prior to this period was 376 standard m^3/s. In order to meet this demand, a remote set point change in the station discharge pressure control (DPC) was issued from the Gas Control Centre in a manner shown in Fig. 13a. The sequence of compressor unit operations required to drive the unit towards the set point pressure was directed by the on-site station control system which is simplified by the set of controllers shown on the left-hand-side of Fig. 12.

Telemetry and calculated information is updated instantaneously in the Gas Control Centre on a four minute scan basis. A twelve minute average is calculated from three consecutive four minute scans.

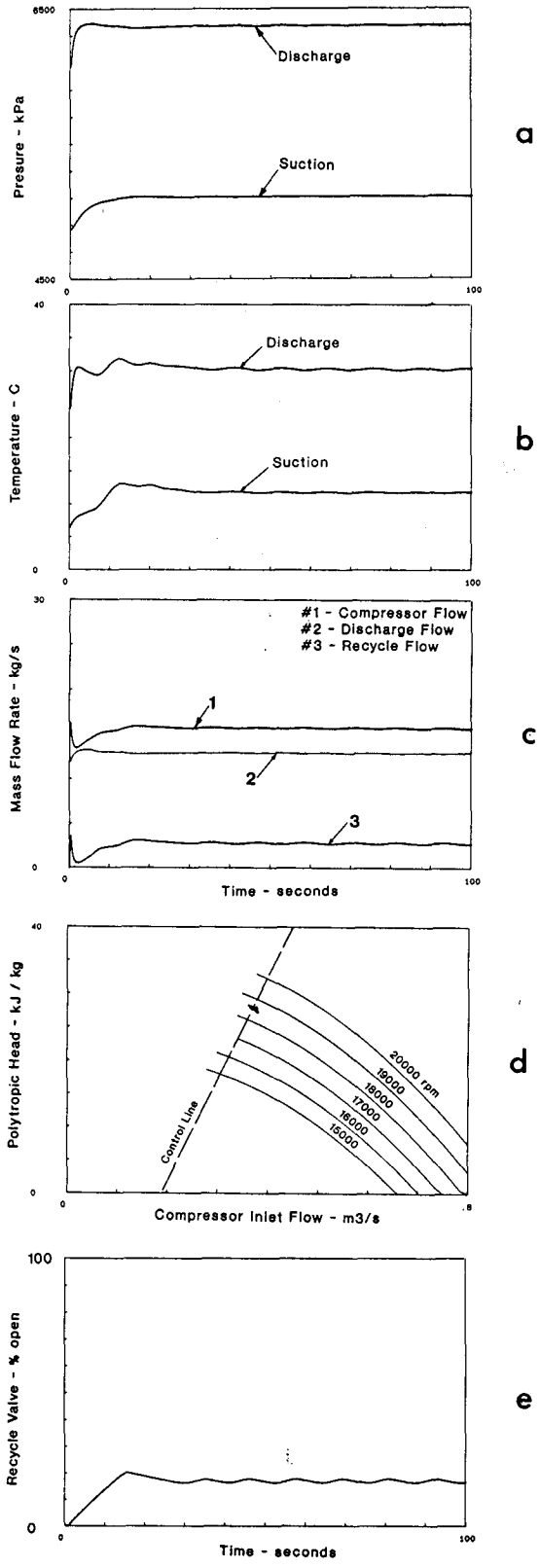

Fig. 9 Simulation results during the process of compressor surge protection (k=0.5).

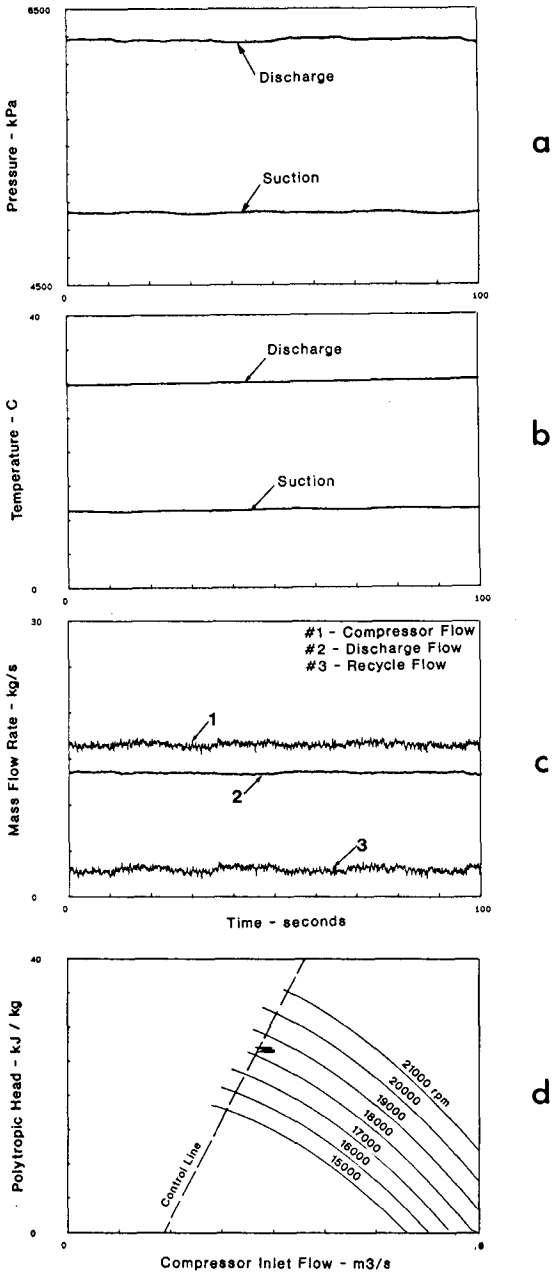

Fig. 10 Field measurements during the process of compressor surge protection (k=0.5).

Figure 14 shows some of the telemeterd data; namely: suction and discharge pressures, station flow measured by the station orifice meter, and the calculated (H_p-Q_a) plot during the same six hour period.

Dynamic simulation for the station configuration including the simplified control system shown in Fig. 12 was conducted. The mainlines upstream and downstream of the facility were simulated via capacitance (volume) and resistance elements. Boundary conditions upstream were taken at constant pressure of 5343 kPa and temperature of 15°C, while at the downstream end, the flow demand of Fig. 13b was imposed. The DPC set point pattern of Fig. 13a was

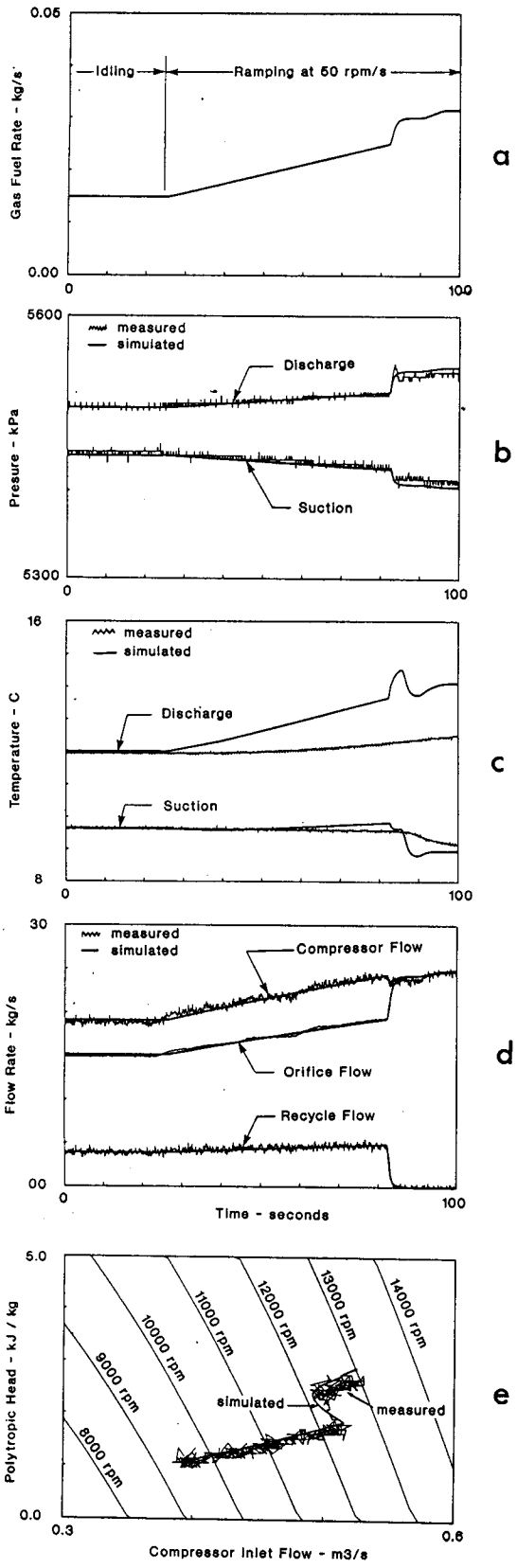

Fig. 11 Comparison between simulation results and field measurements during startup of the compressor of Fig. 4.

then introduced in the simulation and the results obtained are shown in indicative Figures 15. It can be shown that these results compare very favourably with the telemetered information (Fig. 14). The following observations can also be made:

- A very significant peak in station flow follows each major DPC set point increase. This is attributed to the dynamic behavior of the discharge pressure controller and its interaction with other controllers. In this example, due to the large capacitance of the discharge mainline, the discharge pressure cannot follow immediately the DPC and hence a controller error will persist for a while. This will result in increasing the fuel rate to the gas turbine and hence its gas generator speed (see Fig. 15d) to the maximum dictated by the N_G controller. At this time, the N_G controller will take over the control command until the discharge pressure increases (due to packing of the mainline) and the error in the discharge pressure controller decreases. Eventually, the latter controller restores its primary function of controlling the fuel rate to the gas turbine.

- Although the results of the station flow obtained by TRAN and that telemetered are similar, there is a shift in their relative magnitude of approximately 5 - 6 %. This can be attributed to the accuracy of the flow rate measurement by the station orifice meter.

- The peaks in Fig. 14 are somewhat distorted and appear different to those in Fig. 15 due to the difference in resolution. The points in Fig. 14 were taken every twelve minutes while the calculated data in Fig. 15 are every ten seconds.

CONCLUDING REMARKS

Simulation of dynamic gas flow within a compressor station requires mathematical modelling of the gas dynamics of the flow through the compressor and the associated yard piping, together with mathematical descriptions of the control system and turbine driver. The type of equations and method of solution are different for the gas dynamics part than those for the control system, and therefore, dynamic modelling of the station requires two levels of computations that are performed sequentially in a closed loop fashion.

The transfer matrix approach is a useful tool in modelling gas transients in geometrically complicated networks such as those found in compressor station yard piping. Once a transfer matrix is formulated for each element in the system, an overall transfer matrix for the entire network can be easily constructed and subsequently solved with a sparse solver routine.

Good agreement between the simulation results and actual field measurements was obtained.

ACKNOWLEDGEMENT

The work presented here is part of a research project sponsored by NOVA CORPORATION OF ALBERTA and the permission to publish it is hereby acknowledged.

REFERENCES

1. Thorley, A.R.D. and Tiley, C.H., "Unsteady and Transient Flow of Compressible Fluids in Pipelines - A Review of Theoretical and Some Experimental Studies", Heat and Fluid Flow, **8**(1), March (1987).

2. Turner, W.J. and Simonson, M.J., "Compressor Station Transient Flow Modeled", Oil and Gas J., 79-83, May 20 (1985).

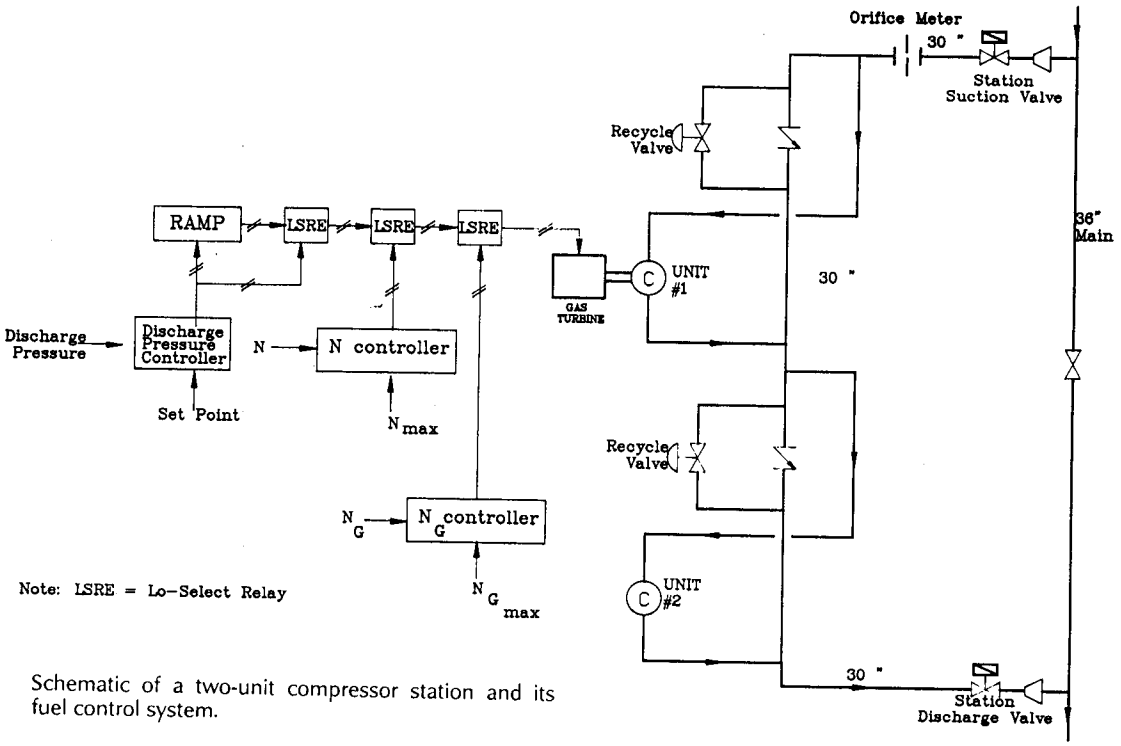

Fig. 12 Schematic of a two-unit compressor station and its fuel control system.

3. Turner, W.J. and Simonson, M.J., "A Compressor Station Model for Transient Gas Pipeline Simulation", Pipeline Simulation Interest Group Annual Meeting, Chattanooga, Tenn., Oct. 18-19, (1984).

4. Bender, E., "Simulation of Dynamic Gas Flows in Networks Including Control Loops", Computers and Chemical Engineering, **3**, 611-613, (1979).

5. Van Zee, G.A., "Control System Design for a Centrifugal Compressor Using Dynamic Simulation", Automatic Control, World Congress, **2**, 363-368, (1987).

6. Boyce, M.P., et. al., "Tutorial Session on Practical Approach to Surge and Surge Control Systems", Proceedings of the 12th Turbomachinery Symposium, Texas A&M University, 145-173, (1983).

7. Stanley, R.A. and Bohannan, W.R., "Dynamic Simulation of Centrifugal Compressor Systems", Proceedings of the 6th Turbomachinery Symposium, Texas A&M University (1977).

8. Picard, D.J. and Bishnoi, P.R., "The Importance of Real-Fluid Behaviour and Nonisentropic Effects in Modelling Decompression Characteristics of Pipeline Fluids for Application in Ductile Fracture Propagation Analysis", Can. J. Chem. Eng., **66**, 3-12, Feb. (1988).

9. Issa, R.I. and Spalding, D.B., "Unsteady One-Dimensional Compressible Frictional Flow With Heat Transfer", J. Mech. Eng. Sciences, **14**(6), 365-369, (1972).

10. Beam, R.M. and Warming, R.F., "An Implicit Finite-Difference Algorithm for Hyperbolic Systems in Conservation Law Form", J. Comp. Phys., **22**, 87-110, (1976).

11. Botros, K.K., Mah, D.B. and Campbell, P.J., "Dymanic Simulation of Compressor Station Installations Including Control Systems", Pipeline Simulation Interest Group Annual Meeting, El Paso, Texas, Oct. 19-20, (1989).

12. Schultz, J.M., "The Polytropic Analysis of Centrifugal Compressors", J. of Engineering for Power, Transaction of ASME, 69-82, January (1962).

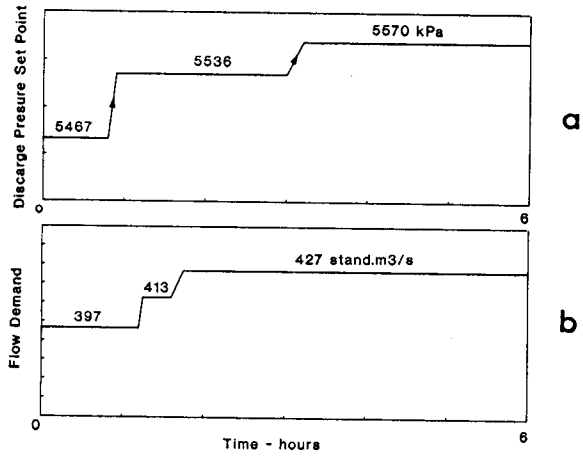

Fig. 13 Discharge pressure control and flow demand for a six hour period.

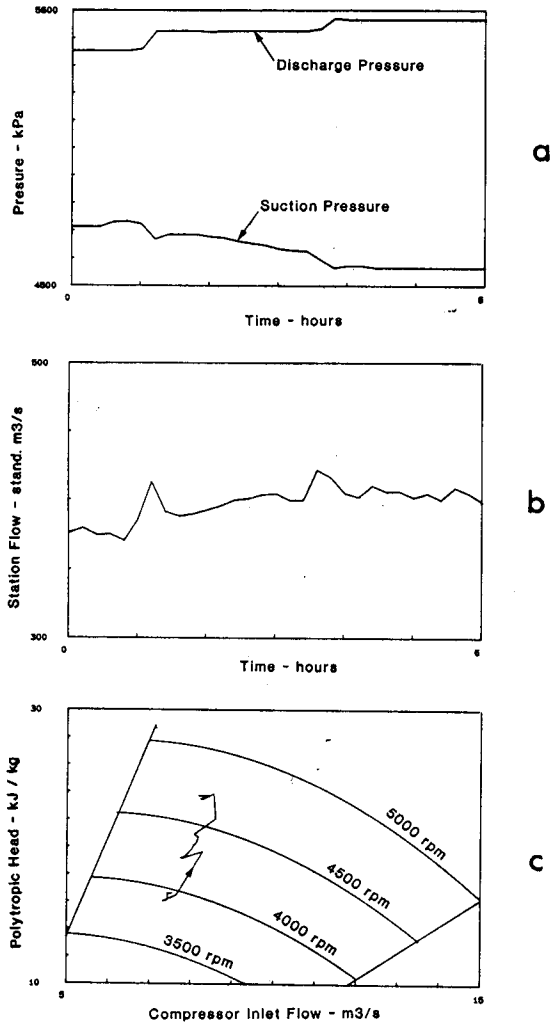

Fig. 14 Twelve (12) minute average telemetry and calculated information during the six hour period of Fig. 13.

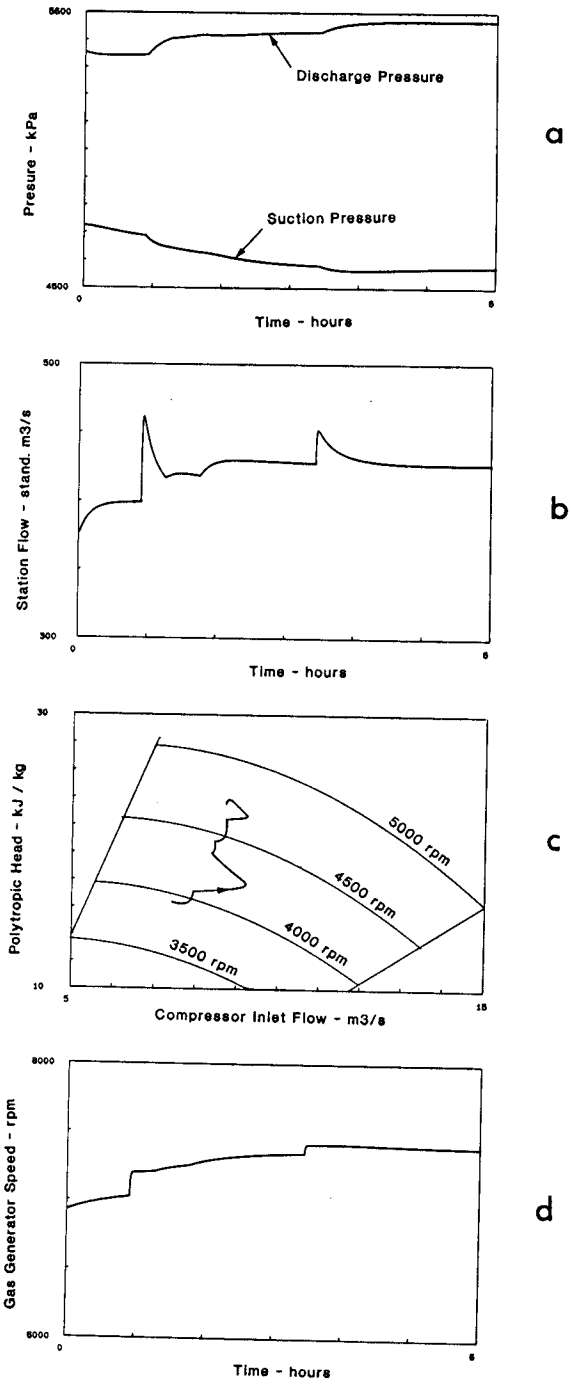

Fig. 15 Simulation results during the six hour period.

13. Duff, I.S., "MA28 - A set of FORTRAN subroutines for Sparse unsymmetrical Linear Equations", Computer Sciences and Systems Division AERE HARWELL, R. 8730, Oxfordshire, England, November (1980).

14. Audry-Sanchez, J., "On the Numerical Solution of Differential Algebraic Equations", Can. J. Chem. Eng., **66**, 1031-1035, December (1988).

15. Gear, C.W., "Numerical Initial Value Problems in Ordinary Differential Equations", Prentice Hall, Inglewood Cliff, N.Y., (1971).

16. Van der Houwen, P.J., "Construction of Integration Formulas for Initial Value Problems", North Holland Publishing Company - Amsterdam, New York, Oxford (1977).